Chapter 3
Practical Aspects of Steady-State Stability Assessment in Real-Time

José Santos Vergara Perez, Tran Anh Thai, Nguyen Duc Cuong, Horia S. Campeanu and Savu C. Savulescu

Abstract Amid the many practical aspects of performing steady-state stability assessment in real time, this chapter addresses the: accuracy testing of the approach, tracking of the distance to instability on Supervisory Control And Data Acquisition (SCADA) trending charts, and the ability to compute the instantaneous voltage and angle stability sensitivities by using Phasor Measurement Unit (PMU) data. The validation of the stability reserve predicted by the stability software and its tracking on SCADA trending charts are illustrated with actual examples taken directly from early QuickStab user sites prior to the June 2010 acquisition of this software by Siemens AG, Nuremberg, Germany. The use of phasor measurements, which, although conceptually different from the conventional SCADA data model, can help assess the voltage and angle stability sensitivities when large blocks of power are transferred across long transmission lines, is exemplified by a successful experiment conducted in Vietnam. Additional considerations are provided to make the case for deploying steady-state stability tools in real time.

S. C. Savulescu (✉)
Energy Consulting International, Inc., 405 Lexington Avenue, 26th Floor, New York, NY 10174, USA
e-mail: savu@eciscs.com

J. S. V. Perez
Empresa de Transmisión Eléctrica, S.A., Panama, USA

T. A. Thai
Advanced Technical Systems Co., Ltd., Hanoi, Vietnam

N. D. Cuong
National Power Transmission Corporation, Hanoi, Vietnam

H. S. Campeanu
ISPE, Bucharest, Romania

S. C. Savulescu (ed.), *Real-Time Stability in Power Systems,*
Power Electronics and Power Systems, DOI 10.1007/978-3-319-06680-6_3,

3.1 Introduction

Speed, reliability, and ease of use are key requirements that any software meant to run in a control center must meet. These attributes are even more critical for programs that perform complex algorithms and entail extensive user interaction, e.g., network analysis applications such as load flow and state estimation. Stability assessment is no exception. In order to qualify for being deployed in real time, the stability software must, of course, be fast, reliable, and easy to use—but, unlike other network analysis applications, which fit naturally in a SCADA/EMS, it invites special scrutiny to appraise its ability to identify, quantify, and visualize the *stability limits,* as opposed to just determining whether a given condition is stable or unstable.

Many, if not most, stability programs available until a few years ago, would not pass this test. They "determine whether a given condition is stable or unstable, [but] have not been efficient in quickly and automatically determining the stability limits" (Kundur 1999).

Actually, Professor Kundur's statement was an understatement, in the sense that the very concept of "stability limit" he was talking about was used loosely and without being quantified not only in this widely quoted reference but also in the vast majority of the papers available at that time and/or published afterwards.

So, then, what *is* "stability limit?"

Theoretically, it is a local property of the system state vector: For each new system state, there are one or several stability limits. Simply stated, "stability limits" exist, are not fixed, and change with the total MegaWatt (MW) system grid utilization,[1] voltages, topology, and the path (trajectory) followed to approach them. Due to their changing nature and assuming that a metric has been defined to quantify them, the "stability limits" need to be recomputed *quickly* and *as often as possible*. This is because, when the system is close to instability, the collapse happens instantly and leaves no time to react.

Therefore, in addition to a *metric* that would *quantify* the stability limits, there is also a need to *rapidly reevaluate* such limits—after each state estimate and after each load flow. In fact, North American Electric Reliability Corporation's (NERC) Policy 9 (NERC 2000) required that reliability coordinators compute the "stability limits" for the current and next-day operation processes to "foresee whether the transmission loading progresses or is projected to progress beyond the operating reliability limit."

Was this being done after NERC released its injunction?

The wave of blackouts that affected US, UK, and mainland Europe utilities in 2003 and 2004 suggests that this was not the case, perhaps because detecting thermal and voltage violations was straightforward whereas defining, identifying, and

[1] When the system is importing power, the total MW system grid utilization is calculated by summing up the total MW generation with the total imported MW; when exporting power, the total MW system grid utilization is the total generated MW. In other words, this number shows how many MW are currently "circulating" in the transmission system.

computing stability limits in real time were an altogether different problem that conventional stability methods did not and could not solve. Moreover, since dispatching a power system without knowing its actual stability limit was like walking on thin ice, a "fresh" approach to this difficult challenge was needed.

Actually, such a "fresh" approach had already been at hand since the early 1960s under the umbrella of *steady-state stability,* as this paradigm was understood at that time, and consisted of determining the *stability reserve,* i.e., the distance from any given operating point to the state where voltages may collapse and units may lose synchronism, by alternately evaluating a steady-state stability criterion and computing successively worsened system states. Although the speed, precision, and potential for visualization of this solution technique[2] were known for a long time (Magnien 1964; Moraite et al. 1966; Dimo 1975), a true production-grade implementation of this technology became available only in 1994 with the advent of QuickStab®.[3]

At the outset, however, let us make it clear that by "steady-state stability" we refer to the *classical concept* described by Crary (1955), Anderson and Fouad (1990), and IEEE (1982), as opposed to "small-signal stability" as it is understood nowadays (IEEE/CIGRE 2004). The appeal of steady-state stability paradigm is unique. By using the *practical stability criteria* (Venikov 1977) in conjunction with a conveniently designed network equivalencing scheme (Dimo 1975), it allows quantifying the system-wide stability index called *stability reserve,* local sensitivities $\Delta V/\Delta P$ and $\Delta\delta/\Delta P$[4] that apply explicitly, without system reduction, to selected topologies such as long transmission lines that accommodate the transfer of significant blocks of MW power.

In the following, from the myriad of practical issues related to performing steady-state stability assessment in real time, we will address just three important aspects:

- Accuracy testing and validation of the software tool that implements the steady-state stability algorithm, which, in this case, is Dimo's method.
- Integration of the stability software, in this case QuickStab, with a third-party SCADA/EMS and the real-time tracking of the stability reserve on SCADA displays and trending charts.

[2] Introduced by Paul Dimo in 1961 (Dimo 1961) and addressed extensively in Savulescu (2005, 2009) and related references.

[3] Introduced in 1994 by Savu C. Savulescu, this software was first deployed in real time at Companhia de Transporte de Energia Elétrica de São Paulo (CTEEP) in 1999. Continuously improved solutions followed at OPSIS (Venezuela), ETESA (Panama), Transelectrica (Romania), Independent System Operator in Bosnia and Herzegovina, Transmission System Operator of Serbia, AzerEnerji (Azerbaijan) and LIPA (New York, USA), and were documented in Savulescu (2004, 2009a), Campeanu et al. (2006), Virmani et al. (2007), Arnold and Hajagos (2009), Vickovic and Eichler (2009). This tool is now owned by Siemens and its commercial name is *Siemens Spectrum Power QuickStab*. The software is seamlessly integrated with the Spectrum Power SCADA/EMS platform and SIGUARD® Dynamic Security Assessment suite.

[4] Not to be confused with the dP/dV and $dP/d\delta$ "practical steady-state stability criteria" (Venikov 1977; Dimo 1975; Savulescu 2005, 2009b).

- Use of the phasor measurements provided by Phasor Measurement Units (PMUs) deployed at both ends of a long transmission line to compute explicitly, without using state estimation results, the steady-state stability of the MW transfer across the line.

3.2 Accuracy Testing and Validation

3.2.1 Background

The very nature of stability applications makes it difficult, if not impossible, to check the accuracy of their predictions: Conceptually, it is not possible to depict instability, which is a system state that does not exist. In the case of QuickStab, further complexities arise if one attempted to compare it with conventional stability applications. This is because QuickStab computes the *distance to instability,* whereas conventional stability programs can only say whether the system is stable or not but *do not quantify* the distance to the state where voltages would collapse and generators would lose synchronism.

Recognizing the need to thoroughly test the application before relying on it, the National Dispatch Center (CND) of Empresa de Transmisión Eléctrica S.A. (ETESA), Panamá, where, in 2002, QuickStab was deployed in real time on the SCADA/EMS by Bailey Network Management, Inc. (today Ventyx-ABB, Inc.), and the National Load Dispatch Center (NLDC) of Vietnam Electricity (EVN), Vietnam, where QuickStab has been used off-line since 2004 in system dispatching and operations planning functions, used a systematic approach to perform accuracy and consistency tests.

3.2.2 Load Flows and Instability

It is well known that near the stability limit of a power system, voltages are low and load flows may diverge (Venikov et al. 1975). However, a nonconverging load flow does not necessarily imply system instability. It was demonstrated that the system load where the load flow diverges is just an upper bound, for one or several units may lose synchronism before that point (Sauer and Pai 1990; Vournas et al. 1996).

The situation is quite interesting. On the one hand, "for voltage collapse and voltage instability analysis, any conclusions based on the singularity of the load-flow Jacobian would apply only to the voltage behavior near the state of maximum power transfer. Such analysis would not detect any voltage instabilities associated with synchronous machines characteristics and their controls" (Sauer and Pai 1990, pp. 1380).

On the other hand, running load flows at increasingly high load levels until divergence is the only way to obtain a base case near the limit of stability, which

then could be used as a starting point by stability assessment tools to perform voltage, steady-state, and/or transient stability checks. This suggests that by alternately performing load-flow calculations and stability checks, one can verify, at least approximately, that the system conditions predicted at, or near, instability correspond to an unsolvable state.

3.2.3 Methodology

The QuickStab accuracy testing procedure, which can be used to validate any type of stability software that has the ability to quantify stability limits, involves using QuickStab in conjunction with a pair of reliable load flow and transient stability programs (in this case, the Siemens PTI PSS/E) as follows.

Given a state estimate or a solved load-flow solution of a power system network, QuickStab computes, in addition to several other indicators, the total MW system grid utilization and the MW generation schedules for the:

- *Critical state* where voltages collapse and units may lose synchronism
- *Security margin* state that corresponds to a user-defined *x*% security margin, typically 15 % below the critical state

The goal is to demonstrate that critical states are indeed critical, and that the *x*% parameter, e.g., 15 %, used for the security margin is adequate.

The critical MW is not a fixed, permanent constant. It depends upon the topology, reactive compensation, and voltage schedules in the system state being evaluated. It is larger if the case entails high bus voltages and large amounts of reactive sources, and it is smaller when voltages are lower and the reactive sources are fewer. Therefore, the validation must encompass both normal and contingency system states over a broad range of system load, network topology, bus voltages, and reactive compensation scenarios.

3.2.3.1 Testing the Accuracy of the Critical State Predictions

When running a load-flow calculation with the MW generation schedules computed for the critical state, one of the following mutually exclusive outcomes should be expected:

a. The load-flow solution converges and either produces a state that QuickStab identifies as being critically stable[5] or, by slightly further increasing the load, produces an unstable state.
b. The load-flow solution produces a state that QuickStab finds to be unstable.
c. The load flow diverges, in which case the generation of MW schedules has to be reduced until a proper solution has been obtained.

[5] In QuickStab parlance, a state is "critically stable" if its steady-state stability reserve is < 1 %.

Therefore, the idea is to compare the stability limits *predicted* for the base case with the stability limits *actually computed* from a load-flow solution that is known to be near instability and to repeat the procedure for different system MW and voltage levels.

Step 1 of the testing procedure entails solving a base caseload flow for peak-load level conditions.

Step 2 consists of running QuickStab for the base case and then retrieving the:

- MW output of the generators for the critical state
- MW output of the generators for the security margin state corresponding to a steady-state stability reserve of 15 %

Step 3 entails running a new load flow, called "critical state load flow", by using the generators' MW predicted for the critical state in the base case. If the critical state load-flow converges, then:

- Run QuickStab—the expectation is that this case will be found either unstable or critically stable
- Increase the slack-bus generation while maintaining the critical state MW schedules and run new load flow(s) until the load-flow program diverges
- Run QuickStab for the system conditions produced by the most recent converged load flow—this case should be found unstable

If the critical state load flow diverges, reduce the slack-bus generation in small increments until convergence has been reached, then:

- Run QuickStab again—this case should be found either unstable or critically stable.
- Reduce by 1 % the total generation and run a new load flow, then execute the stability calculations—this case should be found either critically stable or stable but close to the stability limit.

Since at smaller MW grid utilization levels, which entail less reactive compensation, the stability limits are expected to be lower, the Steps 1 through 3 should be repeated for medium–high and medium–low load levels.

3.2.3.2 Validating the Security Margin

The security margin state corresponds to a *safe* total MW system grid utilization, or *security margin,* such that, for any system state with a stability reserve smaller than this value, no contingency, either single or multiple and no matter how severe, would cause transient instability (Magnien 1964; Moraite et al. 1966; Savulescu 2005). The security margin is related to the stability limit associated with a particular system state and is a by-product of the computations described in Sect. 3.3.1. The accuracy of its prediction can be validated as follows:

- Calculate "security margin load flows" by using the generators' MW schedules predicted by QuickStab for peak, medium–high, and medium–low load cases.
- Run QuickStab for the "security margin load flows" and compare the results.

Please note that, just like the critical MW system grid utilization, the security margin, expressed as a percentage below the critical MW, is not a universal constant. It depends upon the specific combination of topology, load amounts and locations, generators, and reactive compensation, and must be determined and periodically reassessed for each particular transmission system through extensive transient stability simulations.

The expected outcomes of such transient stability calculations are as follows:

a. For load-flow cases with total MW system grid utilization levels *higher than the security margin,* at least one fault or contingency should result in transient instability.
b. For load-flow cases at the *critical MW* level, all the faults and contingencies cases should be unstable.
c. For load-flow cases where the system MW load is *equal to, or below the security margin,* all the fault and contingency cases should be stable.

However, transient stability calculations are time consuming and require significant effort to prepare the data and set up the study cases. If, for practical reasons, the accuracy testing must be kept to a reasonable level, a shorter computational sequence can be followed as follows:

- Identify a relatively small number of faults and contingencies *known a priori* to correspond to worst-case scenarios.
- Perform transient stability calculations for the base case and the security margin state in the peak-load scenario—skip the critical state because, most probably, all the faults and contingencies would result in transient instability anyway.
- Repeat the procedure for medium–high and medium–low load-level scenarios and run transient stability for the critical states as well.

3.2.3.3 Accuracy Testing for Line Contingency Scenarios

The theory predicts that, during line contingencies, the system gets closer to its stability limit—when lines trip, the overall system equivalent reactance increases and, accordingly, the steady-state stability reserve decreases. If the procedure for testing the accuracy of the critical state predictions was repeated for a contingency case, one should expect that the critical MW in the contingency case would be lower than the critical MW in the base case, i.e., the contingency case would have a smaller steady-state stability reserve and the same should be true for the security margin, too.

Therefore, in order to verify the accuracy of the stability limits predicted for a contingency case, the same validation suite, as executed for a specific load level in the base case, must be repeated by starting at the same load level but from a new

base case that corresponds to a major line contingency. The procedure is then repeated for other contingencies and load-level scenarios.

3.2.4 The Panamanian Experience[6]

Until recently, ETESA's CND was equipped with a SCADA/EMS[7] that incorporated, in addition to an extended array of network analysis functions, a real-time version of QuickStab. The program was seamlessly integrated with the real-time network analysis sequence and was used both in real time and off-line to monitor the risk of blackout caused by instability.

Although the operating reliability measures adopted at CND had prevented major disturbances, nearly critical situations have occurred, as it was the case on August 22, 2002, when the system experienced low voltage conditions. The situation was quickly identified and successfully acted upon by the system operator and security engineers. As shown in Gonzalez (2003) and Vergara et al. (2005), QuickStab was used to assess *post facto* the incident and correctly determined that the system was indeed approaching conditions that could have caused a blackout. With the advent of the coordinated operation in Central America, it was felt that the impact of significant MW transfers in the region would have to be continuously monitored in order to detect and prevent the risk of blackouts. Since operators and security engineers must rely on the predicted distance to instability, CND considered it important to validate the accuracy of the QuickStab computations by comparing their outcome with results from simulations performed with PSS/E.

The calculations were conducted at CND. The power flow modeled the entire interconnected system in Central America but the stability calculations focused only on the actual transmission network of ETESA. The study assumptions were based on the actual operating guidelines adopted at CND, and the QuickStab computational options were set to match the way PSS/E calculates load flows.

3.2.4.1 Load-Level Scenarios

The validation suite used to compare the QuickStab calculation results with PSS/E load-flow computations included the following load-level scenarios:

- *Maximum Expected Demand:* In this scenario, all the shunt capacitors are online, the shunt reactors are disconnected, and a small unit that normally is not needed to generate MW is brought in service to generate MVAr. These reactive

[6] The tables and charts presented in Sect. 2.4 have been reprinted, with permission, from an internal study conducted by the CND.

[7] At the time of this writing, the ETESA's SCADA/EMS was being replaced with a new system that incorporates a different suite of network analysis applications.

compensation sources help meet the highest possible MW load without risk of voltage collapse.

- *Medium–HIgh Demand:* In this scenario, several steps are taken to reduce the reactive compensation: 15 MVAr in capacitor banks are taken off-line, 40 MVAr in shunt reactors are reconnected, and the machine used to generate MVAr is not activated. These provisions in the load-flow setup emulate the CND operating procedures for lower MW levels where the amount of reactive compensation is reduced to ensure that the system voltages would not violate the higher limits.
- *Medium–Low Demand:* This scenario is similar to the medium–high scenario, but at a further reduced MW load level and 15 MVAr less in capacitor banks.

3.2.4.2 Results of the Accuracy Tests Performed at CND

The detailed numerical outcome of the accuracy testing calculations performed at the CND of ETESA is documented in Table 3.1. In order to facilitate the interpretation of the results, which unequivocally attest the excellent precision of QuickStab, they are summarized on charts and further discussed in the following sections.

Maximum Expected Demand Scenarios

Figure 3.1 depicts the main results of the accuracy testing calculations performed for the maximum expected demand scenario. Five cases were developed and analyzed as follows:

- Case 1: 957 MW base case calculated with PSS/E. The QuickStab application predicted that instability, i.e., the critical state, occurs at 1018 MW, with a security margin of 15 % at 861 MW, and calculated critical MW schedules for the critical state and security margin MW schedules for the security margin state.
- Case 2: PSS/E *diverged* with the critical MW schedules from Case 1. The slack-bus generation was then slowly decreased, while maintaining all the other MW generation schedules unchanged, until convergence was obtained at 1007 MW. The fast voltage and steady-state stability application evaluated this case as unstable. The concept of security margin does not apply when the state is unstable, and, therefore, it was not calculated.
- Case 3: A new PSS/E load flow was executed by reducing the slack-bus generation by 10 MW, i.e., approximately 1 %. The case converged at 995 MW. For this case, QuickStab determined that the system is critically stable with a stability reserve of 0.91 % from the new limit of stability of 1005 MW. The security margin for Case 3 was evaluated at 850 MW.
- Case 4: The MW generation in Case 4 was further reduced by another 1 % to 983 MW. QuickStab determined that the system is stable, with 2 % stability reserve, and predicted that instability occurs at 995 MW. The security margin for Case 4 was evaluated at 842 MW

Table 3.1 Total MW, average system voltage, and steady-state stability reserve for the maximum expected, medium–high and medium–low demand scenarios

Study case		State	Total MW	Average system voltage	Stability reserve [%]	
Expected maximum demand: Cases 1 through 4	Base case	Actual	957	1.0487	6.07	*Stable*
		Security margin	861	1.1167	15.34	
		Critical	1018	0.9723	0	
	Critical MW	Actual	1008	1.0177	0	*Unstable*
		Security margin	n/a	n/a	n/a	
		Critical	1008	1.0177	0	
	Critical MW: 1% less load	Actual	995	1.0406	0.91	*Critically stable*
		Security margin	850	1.0132	15.34	
		Critical	1005	0.9667	0	
	Critical MW: 2% less load	Actual	983	1.0498	1.12	*Stable*
		Security margin	842	1.1442	15.79	
		Critical	995	1.0388	0	
Medium high demand: Cases 1 through 4	Base case	Actual	798	1.0567	12.26	*Stable*
		Security margin	766	1.0377	15.67	
		Critical	909	0.9985	0	
	Critical MW	Actual	906	1.0240	0	*Critically stable*
		Security margin	765	1.1741	15.52	
		Critical	906	1. 0240	0	
	Critical MW raised to divergence	Actual	931	1.0194	0	*Unstable*
		Security margin	n/a	n/a	n/a	
		Critical	931	1.0194	0	
	Base case + new unit for MVAr	Actual	798	1.0567	14.85	*Stable*
		Security margin	763	1.0338	18.56	
		Critical	937	0.9885	0	
Medium–low demand: Cases 1 through 3	Base case	Actual	742	1.0517	15.75	*Stable*
		Security margin	742	1.0517	15.75	
		Critical	881	0.9840	0	
	Critical MW	Actual	881	1.0543	0	*Critically stable*
		Security margin	748	1.1924	15.11	
		Critical	881	1.0543	0	
	Critical MW raised to divergence	Actual	913	1.0175	0	*Unstable*
		Security margin	n/a	n/a	n/a	
		Critical	913	1.0175	0	

- Case 5: The MW generation in Case 5 was set at 861 MW, which corresponds to the 15% security margin predicted for the Case 1. The steady-state stability limit computed by QuickStab was 997 MW.

Medium–High Demand Scenario

Figure 3.2 illustrates the simulation results for the Medium–High Demand scenario. Three cases were analyzed as follows:

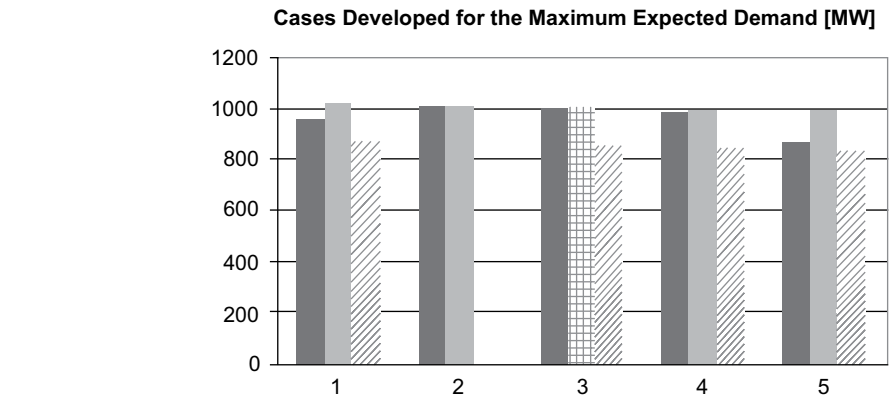

Fig. 3.1 Expected maximum demand cases. All the reactive compensation devices are on line. The system's maximum transfer capability is at its highest value

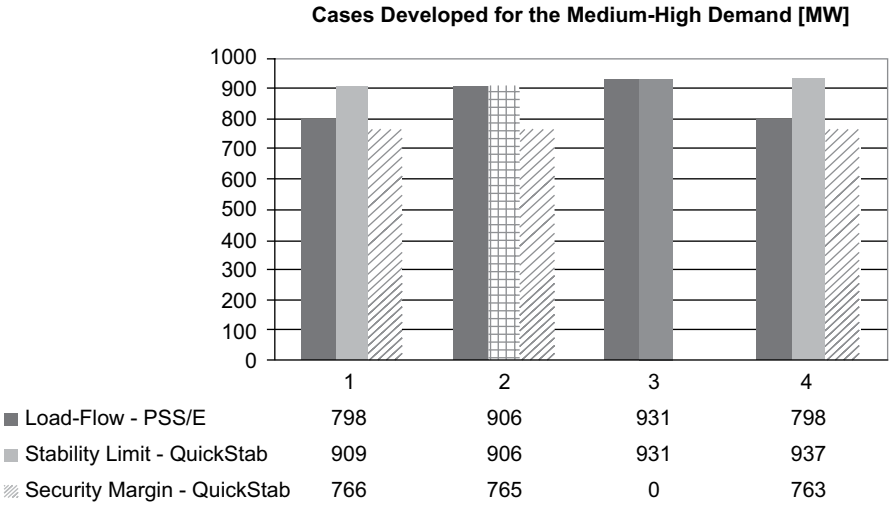

Fig. 3.2 Medium–high demand cases. Fewer reactive compensation devices are on line and, accordingly, the system's maximum transfer capability is lower, too

- Case 1: 798 MW base case load-flow calculated with PSS/E. QuickStab predicts that instability occurs at 909 MW, with 15% security margin at 766 MW, and calculates the MW generation schedules for both the critical and the security margin states.
- Case 2: The PSS/E load flow was executed with the critical MW schedules predicted by QuickStab in Case 2 and converged at 906 MW. This case was evaluated as critically stable. The security margin of Case 2 was 765 MW.

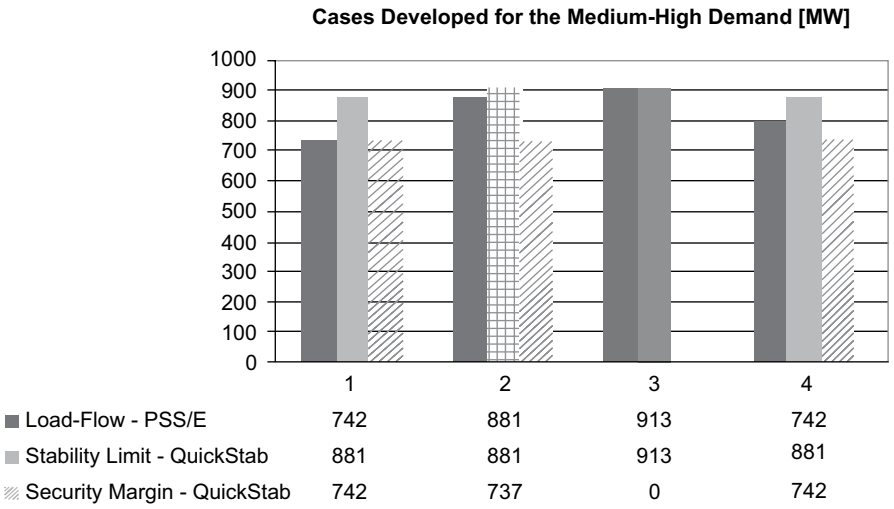

Fig. 3.3 Medium–low demand cases. Most capacitors are disconnected and shunt reactors are on. The system's steady-state stability limit gets even lower than in the preceding cases

- Case 3: A new PSS/E load flow was executed by increasing the generation in small steps at the slack bus, while maintaining all the other MW schedules unchanged, up to the point where the load flow would diverge. The last converged load flow was obtained at 931 MW and evaluated by QuickStab as unstable.
- Case 4: A special case was derived from the Case 1 by including a small machine that did not generate any MW in the base case but was allowed to pick up some load during the case-worsening calculations performed by QuickStab during the search of the steady-state stability limit.

The purpose of running Case 4 was to simulate the actual operating conditions in Panama where, in order to operate the transmission system at higher load levels, the actual practice is to bring this small generating unit online to generate the MVAr needed for reactive compensation. As shown in Fig. 3.2, starting from a 798 MW case, the fast voltage and steady-state stability application correctly predicted a *higher stability limit,* i.e., 937 MW versus the 909 MW in Case 1.

Medium–Low Demand Scenario

The Medium–Low Demand scenario calculation results are shown in Fig. 3.3. The following cases were analyzed:

- Case 1: 742 MW base case load flow calculated with PSS/E. QuickStab predicts that instability (critical state) occurs at 881 MW, with a security margin of 15% at 742 MW, and calculates the MW generation schedules both for the critical state and for the security margin state.

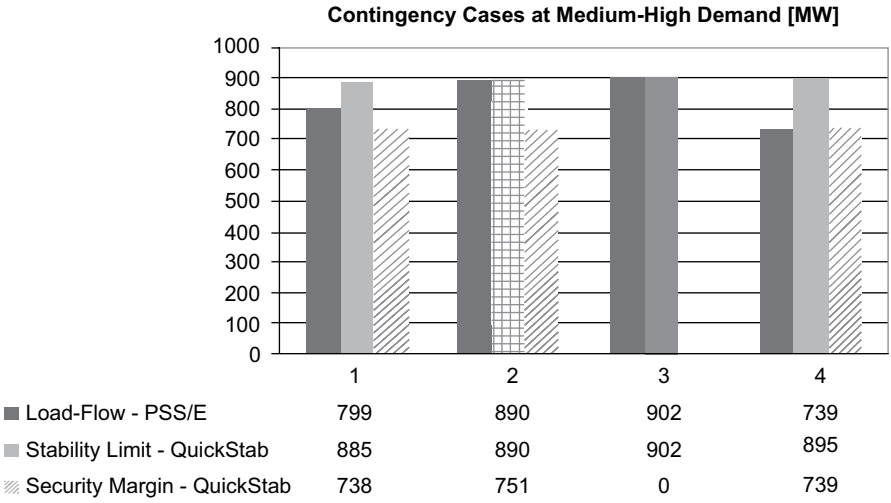

Fig. 3.4 Contingency cases on medium–high demand base case. As expected, the contingency cases have smaller steady-state stability limits when compared with the cases shown in Fig. 3.2

- Case 2: The PSS/E load flow was run with the critical MW schedules predicted by the fast voltage and steady-state stability application in Case 1 and converged at 881 MW. QuickStab evaluated it as critically stable. The security margin was computed at 737 MW.
- Case 3: A new PSS/E load flow was solved by increasing the slack-bus generation in small steps until the load-flow calculations diverged. The last converged solution was at 913 MW and was evaluated as unstable.
- Case 4: This case was supposed to be created with the MW schedules computed for the security margin in Case 1, but since the security margin in Case 1 was already 15 %, Case 4 is identical to Case 1 and is shown in Fig. 3.3 for reference only.

Major Line Contingency

Figure 3.4 illustrates the calculation results for a major line contingency case simulated for the medium–high demand scenario.

Four cases were analyzed as follows:

- Case 1: 799 MW base case load flow calculated with PSS/E. The QuickStab application predicts that instability occurs at 885 MW, with 15 % security margin at 738 MW, and calculates the MW generation schedules for both the critical and the security margin states.
- Case 2: The PSS/E load flow was executed with the critical MW schedules predicted in Case 2 and converged at 890 MW. QuickStab evaluated this case as critically stable. The security margin of Case 4 was evaluated at 751 MW.

- Case 3: A new PSS/E load flow was run by increasing the generation in small steps at the slack bus, while maintaining all the other MW schedules unchanged, up to the point where the load flow would diverge. The last converged load flow was obtained at 902 MW and was evaluated as unstable. The security margin was not calculated.
- Case 4: This case was built with the MW schedules computed for the security margin in Case 1. An 895 MW stability limit was computed, with a 15 % security margin of 739 MW, which was identical to the load-flow case loading.

Transient Stability Simulations

The following transient stability calculation scenarios were evaluated for the Expected Maximum Demand, Medium–High Demand, and Line Contingency Cases:

1. Major generating unit trip in the western area.
2. Major generating unit trip near large load centers.
3. All units of a midsized power plant out of service.
4. Major transmission line contingency.

The results were similar in all the cases and are synthesized as follows:

- *Actual State* (Base Case), corresponding to the "Case 1" conditions described in the previous sections: the system withstood the fault scenarios 1 and 2, but became unstable for the faults scenarios 3 and 4.
- *Security Margin State,* i.e., MW loading 15 % lower than the critical MW in the base cases: the system withstood all the fault scenarios.
- *Critical State,* corresponding to the critic MW in the corresponding base cases: all the transient stability simulations resulted in instability.

3.2.4.3 Analysis of CND Cases

In all the scenarios, QuickStab accurately determined the critical state, regardless of how near or how far it was from the base case. As predicted by theory, the peak-load stability limits were higher than those at medium–high and medium–low load levels. Indeed, in system states with less reactive compensation, we expect that the voltage would collapse at MW levels smaller than the maximum MW loadability of the same network where significant amounts of reactive compensation were added.

In all the cases evaluated, the input load-flow model represented the entire Central American interconnection, but the stability calculations were performed only on the area corresponding to ETESA's transmission network. Accordingly, the program computed MW schedules only for the generators situated in the study area. These MW values were then used in PSS/E to create new load-flow cases, but all the other load-flow data remained the same. The calculations' accuracy thus confirms the usefulness of the multi-area approach used by the program to assess local stability aspects within large interconnections.

Although the amount and extent of the transient stability simulations were rather limited, they did help getting a good understating of the concept of *security margin*. In all the cases evaluated, the system was stable when the transient stability simulations were executed for the security margin system MW grid utilization, but became unstable in various fault scenarios when the system loading was higher than the security margin MW. Furthermore, for all the transient stability calculations performed at the critical system, MW grid utilization level resulted in instability.

As far as the *computational speed* is concerned, all the simulations performed converged instantly, which was actually expected both because the program is intrinsically fast and because the network area that was evaluated for stability was just a subset of the load-flow model of the Central American interconnected power system.

3.2.5 Validating QuickStab Results in Vietnam[8]

Due to frequent and severe faults that, in some cases, have adversely affected system reliability and security, the NLDC of EVN undertook, in 2003 and early 2004, a series of studies aimed at evaluating the risk of blackout caused by instability. Among several initiatives, NLDC assessed the maximum transfer capability of the transmission system by using the QuickStab software.

The analysis revealed that the power system's steady-state stability margins might be inadequate. The stability reserve indices varied from 6 % in the 2005 rainy scenario to 13 % in the 2006 rainy scenario, with a relatively better margin in the dry season of 2006.

Since contingencies would certainly push the system even closer to the steady-state stability limit where voltages may collapse and units may lose synchronism, NLDC concluded that the actual operations of the transmission network for the next couple of years will have to be closely and continuously monitored in order to detect and prevent the risk of blackouts.

Accordingly, NLDC expanded the array of network analysis applications with QuickStab,[9] which, in addition to the then-existing load flow and transient stability programs, was used for some time to support the system dispatching, operations planning, and market clearing functions. The distance to voltage and steady-state instability was calculated three times a day based on the most recent data retrieved from the SCADA/EMS or computed by the market-clearing engine on the Market System.

Since this information had to be relied upon in system and market operations, NLDC developed a series of simulations aimed at validating the accuracy of the QuickStab predictions by following procedures similar to those described in

[8] The tables and charts presented in Sect. 2.5 have been reprinted, with permission, from an internal study conducted by the NLDC.

[9] At the time of this writing, the NLDC's SCADA/EMS is being replaced with a new system that incorporates a different suite of network analysis applications.

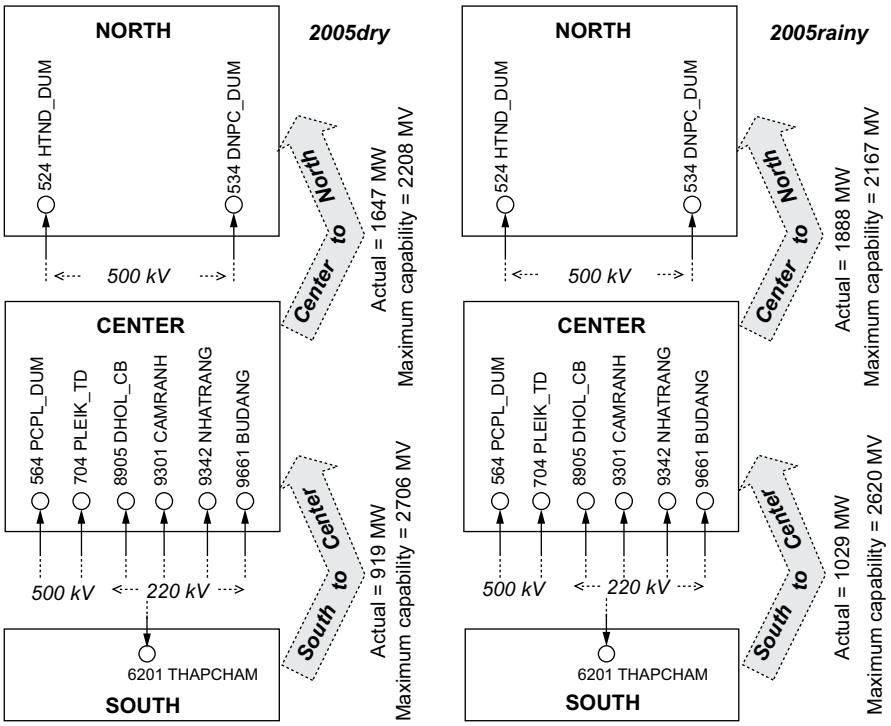

Fig. 3.5 South–North MW transfers in the EVN power transmission network

Sect. 3.3 of this chapter. A brief summary of the most relevant aspects and computational results is provided in the following sections.

3.2.5.1 Testing Scenarios: Simulation Results

The power system of Vietnam has a markedly longitudinal characteristic. It extends over approximately 2000 km and consists of three major subareas, which are loosely interconnected and encompass 220 and 110 kV transmission facilities, attached to an Extra High Voltage (EHV) "backbone" of two 500-kV circuits that go from the extreme south all the way to the northern part of the country (Fig. 3.5).

The operating difficulties that stem from this particular network topology are further worsened by:

- Severe power transfers from the Southern Region to the Northern Region.
- Relatively low load density in the Central Region.
- Large seasonal variations: a *rainy* scenario, where the hydro generation is maximized, and a *dry* scenario, where the generation is primarily thermal.
- Significant MVA injection into the Northern area across the 500 kV lines, disproportionately higher than the flow in the only 220-kV tie-line that interconnects the Northern and Central areas.

Table 3.2 Total MW, average system voltage, and steady-state stability reserve for the dry cases. In sub-scenario A, some generators control voltages at remote buses. In sub-scenario B, all the generators control their own terminals and the overall voltage profile is slightly higher

Study case		State	Total MW	Average system voltage	Stability reserve (%)	
Sub-Scenario A: Cases 1 through 4	Base case	Actual	9516	1.05093	7.17	*Stable*
		Security margin	8699	1.10416	15.14	
		Critical	10,251	0.9450	0	
	Critical MW	Actual	10,250	1.0222	1.17	*Stable*
		Security margin	8754	1.1346	15.60	
		Critical	10,372	0.9699	0	
	Critical MW + 1 % additional load	Actual	10,347	1.0178	0.97	*Critically stable*
		Security margin	8856	1.1299	15.24	
		Critical	10,449	0.9667	0	
	Critical MW + 2 % additional load	Actual	10,447	1.0078	0.71	*Critically stable*
		Security margin	8861	1.11357	15.79	
		Critical	10,522	0.9698	0	
Sub-Scenario B: Cases 5 and 6	Base case	Actual	9494	1.0783	7.8	*Stable*
		Security margin	8717	1.1246	15.34	
		Critical	10,296	0.9389	0	
	Critical MW	Actual	10,488	1.0402	1.22	*Stable*
		Security margin	8926	1.1434	15.93	
		Critical	10,617	0.9828	0	

- There are no shunt capacitors: due to insufficient reactive compensation, the generating units are used to hold voltages at remote locations.

Two scenarios were used for performing the accuracy testing: *Dry* and *Rainy*. Both of these scenarios were built for peak load conditions and evaluated under two voltage control assumptions as follows:

- Some generators are allowed to control remote buses.
- All the generators control their own terminal bus voltages.

The results of the simulations performed for the "dry" cases, where two additional cases were run by successively increasing the load in the critical state load-flows by 1 %, are shown in Table 3.2 and illustrated in Fig. 3.6.

The results of the calculations performed for the "rainy" cases are shown in Table 3.3 and illustrated in Fig. 3.7.

3.2.5.2 Analysis of NLDC Cases

At the outset, it must be noted that, regardless of the study scenario, it was not possible to obtain converged critical state load flows with voltage profiles similar to the ones predicted for the critical state QuickStab.

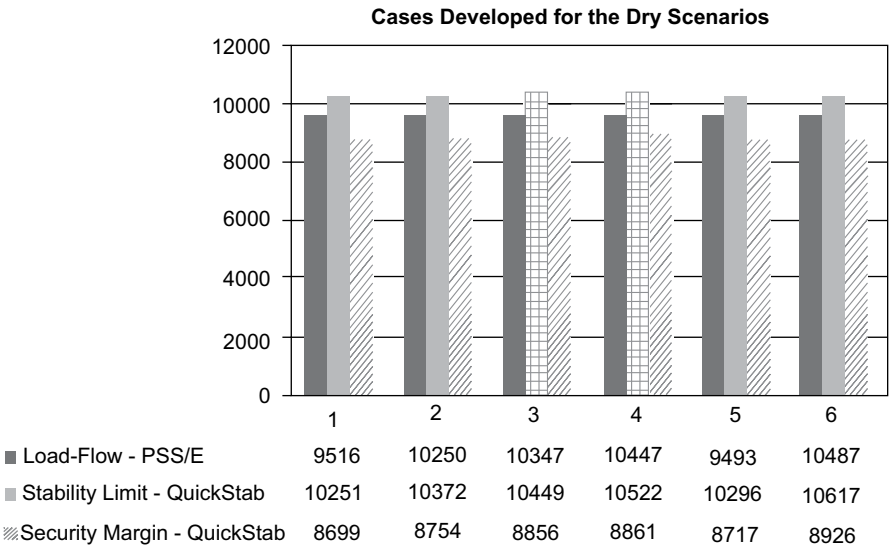

Fig. 3.6 Dry scenario cases

Table 3.3 Total MW, average system voltage, and steady-state stability reserve for the rainy cases. In sub-scenario A, some generators control voltages at remote buses. In sub-scenario B, all the generators control their own terminals and the overall voltage profile is slightly higher

Study case		State	Total MW	Average system voltage	Stability reserve [%]	
Sub-scenario A: Cases 1 and 2	Base case	Actual	9008	1.0857	10.53	*Stable*
		Security margin	8535	1.1108	15.23	
		Critical	10,068	0.9377	0	
	Critical MW	Actual	10,063	1.0368	1.02	*Stable*
		Security margin	8546	1.1399	15.95	
		Critical	10,167	1.0234	0	
Sub-scenario B: Cases 3 and 4	Base case	Actual	8983	1.1012	11.87	*Stable*
		Security margin	8654	1.1081	15.10	
		Critical	10,193	0.9261	0	
	Critical MW	Actual	10,206	1.0344	0.55	*Critically stable*
		Security margin	8698	1.1371	15.25	
		Critical	10,263	1.0270	0	

Whatever might be the reason(s), the fact that the starting system voltage profile in the critical state load-flow cases was higher suggests that the corresponding maximum transfer capability would also be higher, i.e., the system would still have a small steady-state stability reserve, perhaps close to, or slightly below, 1 %, thus qualifying the state as critically stable.

In all the scenarios, QuickStab accurately determined the critical state, regardless of how near or how far it was from the base case. However, the precision was not as good as the accuracy of the Panamanian experiments. A possible explanation,

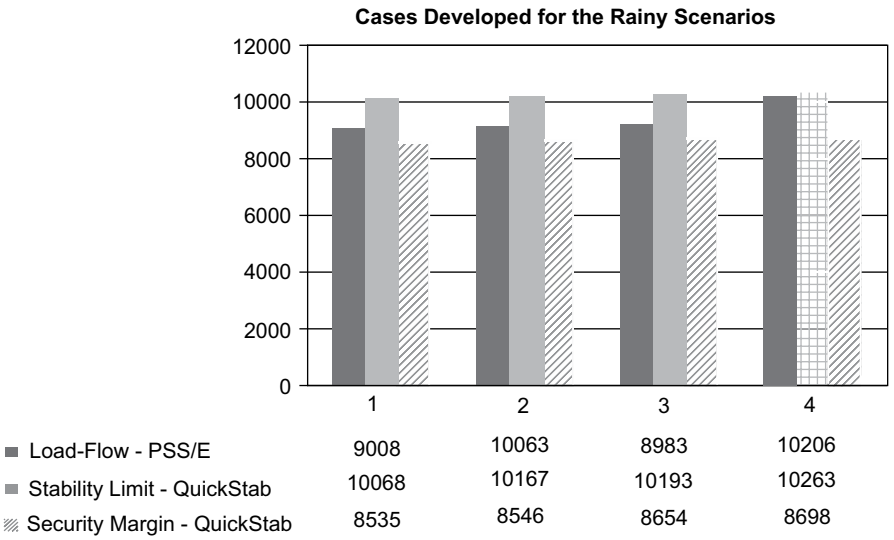

Fig. 3.7 Rainy scenario cases

as suggested in the opening paragraph of this section, might be the fact that in all the "critical MW load flows", the voltages were higher than the target voltage profile, which obviously should bias the calculation results towards higher stability limits, as predicted by theory.

The load-flow model encompassed the complete interconnected power system of Vietnam, but in order to keep the effort involved in simulations to a reasonable level, only the system-wide cases were considered for testing by running load-flow computations near the stability limits and repeating the voltage and steady-state stability calculations for these new cases.

In real life, however, stability calculations are routinely performed on a subsystem, or area, basis. For the Northern Region, which usually imports a significant amount of power from the Central Region, production grade studies revealed that the MW flows in the 500-kV circuits reach the steady-state stability limits way before getting even close to the thermal limits.

For practical purposes, this means that the system operator should monitor not only the steady-state stability reserve but also, and most importantly, the amount of power being transferred into the Northern Region across the 500-kV interconnection.

For the Southern Region, area-level stability simulations have indicated generation capacity limitations, which means that in the south, for the reactive compensation levels normally considered in operational studies, the system is steady-state stable even if all the generators have reached their maximum MW limits. As far as the Central Region is concerned, the load is relatively low and no stability problems are anticipated.

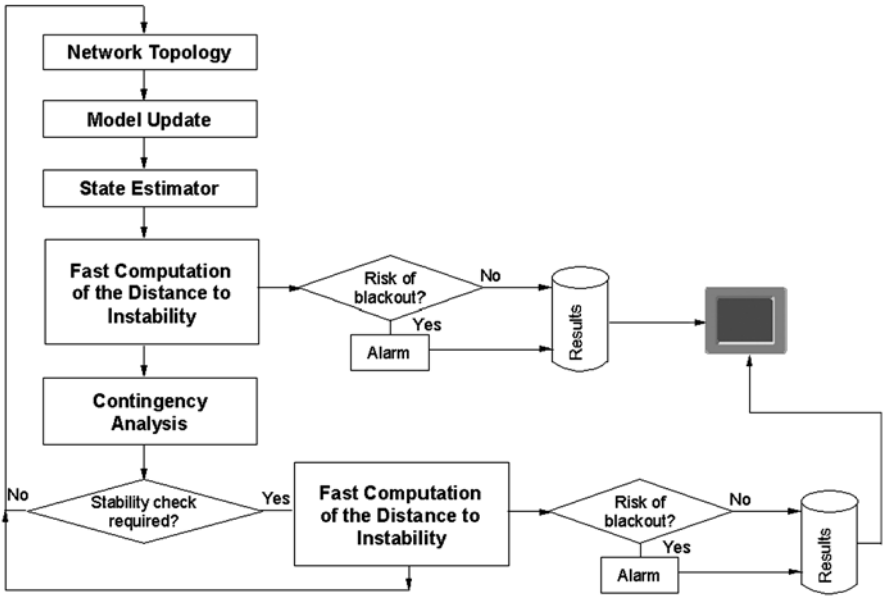

Fig. 3.8 Real-time integration of the fast voltage and steady-state stability analysis computations with the SCADA/EMS state estimator at Transelectrica, Romania

3.3 Tracking the Steady-State Stability Reserve on SCADA Trending Charts

3.3.1 Real-Time Implementation of QuickStab on the SCADA/EMS of Transelectrica

The steady-state stability framework that allows computing and monitoring the distance to instability has been developed, and is well known, in Romania for a very long time (Dimo 1961, 1975), but a true production-grade embodiment of this technology became available only in 2002 when QuickStab was implemented in real time on the SCADA/EMS of Transelectrica,[10] Romania, by Alstom (Avila-Rosales and Giri 2004).

Figure 3.8 illustrates how the QuickStab computational engine that determines the voltage and steady-state stability reserve was seamlessly integrated within the real-time network analysis sequence.

The program is triggered automatically after each successful run of the state estimator and determines both the current value of the system-wide stability reserve

[10] At the time of this writing, QuickStab was being used in real time at the National Dispatch Center (DEN) in Bucharest, Romania, as shown in this section. However, neither the authors of this chapter nor the editor of this book make any implied or explicit assumptions about the continuing use of this application at Transelectrica in the future.

and the steady-state stability reserve for each one of the five critical security cut-sets identified for the Romanian transmission system.

3.3.1.1 Critical Security Cut-Sets

A "security cut-set" identifies a group of transmission lines:

- That form a topological cut-set, i.e., their removal causes the islanding of the transmission network in two disjoint components.
- Whose maximum transfer limit in terms of stability is smaller than the aggregate thermal limit, i.e., may cause voltage and steady-state instability even if the total MW flow across the cut-set has not reached the combined maximum MVA of the lines.

In a sense, the concept of "security cut-set" is similar to the concept of "congestion path" with the difference that the former stems from stability considerations whereas the latter is driven by thermal violations.

Security cut-sets may appear in any multi-area power system where large MW blocks are transferred between areas across relatively weak internal interconnections. This is common in longitudinal transmission networks that span system areas with significant load-generation unbalances, e.g., the Vietnamese power transmission system depicted in Fig. 3.5 where the topologically clustered Northern, Central, and Southern regions are separated by such security cut-sets.

In Romania, where the populated areas and industrial zones are aggregated in concentric areas divided by the Carpathian mountain chain, the security cut-sets are generated by the specific pattern of the MW flows between the center area and the outer ring. The center area is surrounded by mountains and encompasses a dense 110-kV network sustained by a 220–400-kV backbone. Around the central area, there is an outer ring of major power plants that inject their output into a strong 220–400–750-kV transmission system.

The power is transferred primarily from south–southwest towards the center, from south–southeast towards the northeastern part of the outer ring, and from the northern part of the central area towards the northeastern part of the outer ring. DEN has identified five critical security cut-sets. The system subareas circumscribed by these critical security cut-sets are not necessarily disjoint, and some of them overlap. They are not fixed, either, and change depending upon the pattern of load, generating reserves, transmission outages, line flows, voltage levels, and reactive resources.

The configuration of the critical security cut-sets is periodically reassessed offline with an application developed in-house that identifies, for a given load-flow solution, all the security cut-sets and computes the steady-state stability reserve index for each one of them. The approach is described in Pomarleanu and Savulescu (2009) and combines an REI-Dimo equivalencing procedure (Dimo 1975; Tinney and Powell 1977; Dy Liacco et al. 1978; Oatts et al. 1990; Savulescu 1981), which assigns one REI generator to each side of the security cut-set, with a steady-state

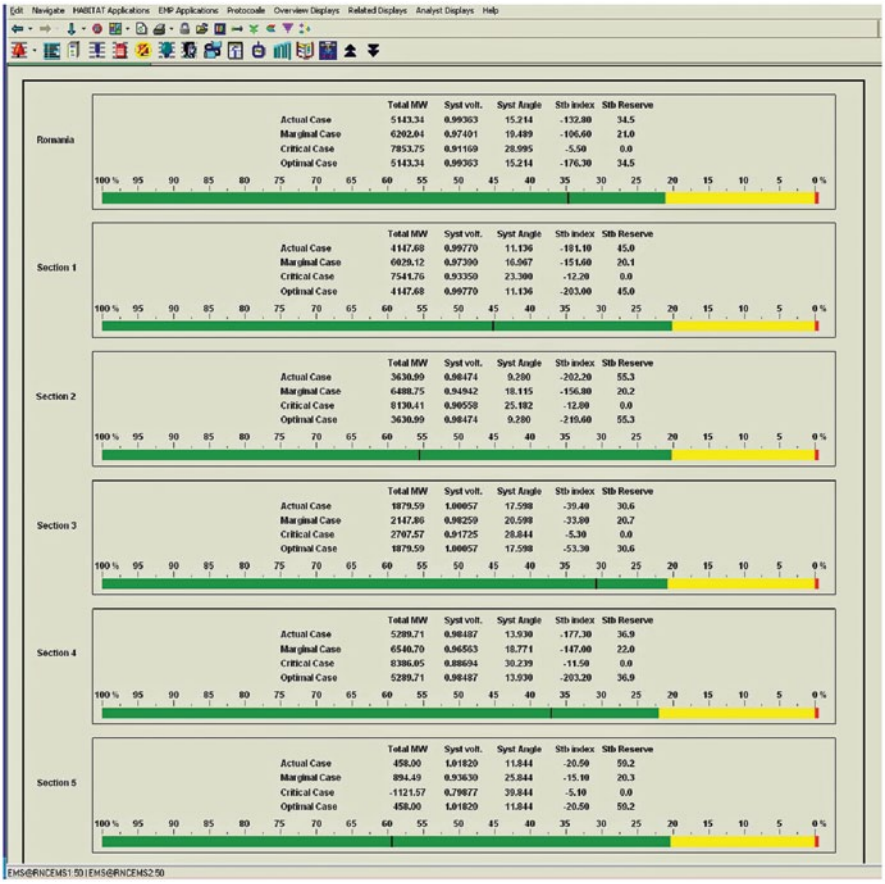

Fig. 3.9 System and security cut-set speedometers. (Reprinted with permission from DEN)

stability calculation for the model consisting of two REI equivalent generators and the link between them.

The security cut-sets are then ranked in the descending order of their steady-state stability reserve and the most critical five are selected. This procedure is executed twice a year. Quite obviously, the actual stability limits across the critical security cut-sets may differ substantially from those computed off-line for the postulated conditions and need to be reassessed continuously based on the actual system conditions as determined by the state estimator. The problem is now solved in real-time QuickStab, which computes the steady-state stability reserves both for the entire system and for each security cut-set. Figure 3.9 shows a real-time display taken directly from the SCADA/EMS, which depicts the current values of the steady-state stability reserves of the system and across the five critical security cut-sets.

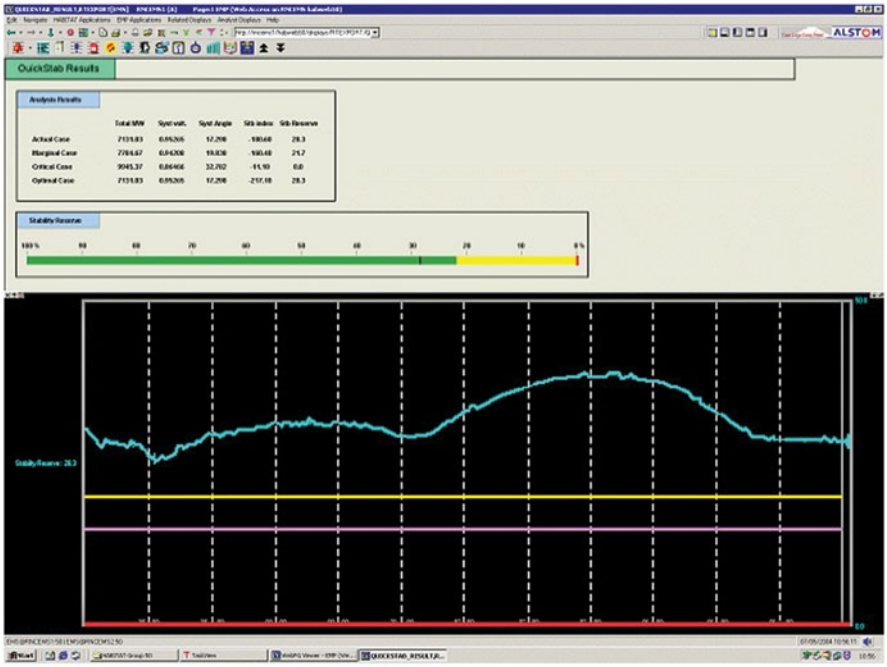

Fig. 3.10 Real-time trending of the distance to steady-state instability on the SCADA/EMS of Transelectrica, Romania. The *light color line* shows the security margin. The *bottom line* corresponds to the steady-state stability limit. The *gray line* in between is the alarm limit. (Reprinted with permission from DEN)

3.3.1.2 Real-Time Trending of the Distance to Instability

The real-time computed values of the system-wide steady-state stability reserve and the steady-state stability reserve of each critical security cut-set is stored in the real-time database and can be subsequently displayed on SCADA trending charts. Figure 3.10 shows a typical trending chart of the system-wide stability reserve over a 24-hour period.

At Transelectrica, Alstom developed an innovative visualization concept, which, on the left side of the monitor, displays the distance to instability for the entire system with each one of the security-cut sets evaluated, and, on the right side, tracks the evolution in time of the stability reserves displayed on the left by using standard SCADA trending charts (Fig. 3.11).

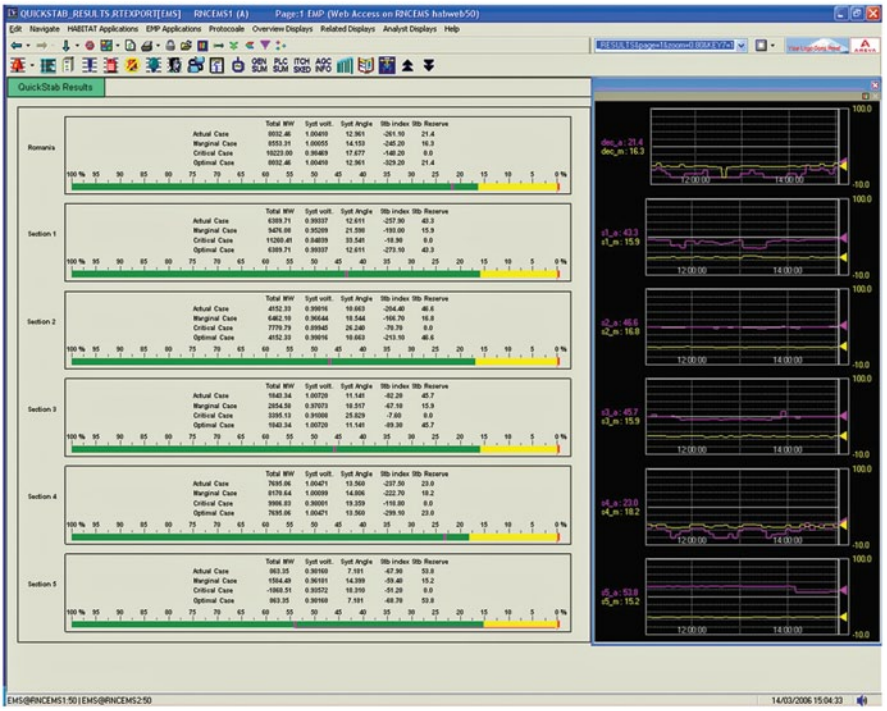

Fig. 3.11 Real-time display from Transelectrica's SCADA/EMS, which combines the linear speedometers with the trending charts. (Reprinted with permission from DEN)

3.4 Using PMUs to Track Voltage and Angle Stability Sensitivities Across Long Transmission Lines in Vietnam

3.4.1 Introductory Background

The need to increase the power transfers across the existing power system infrastructure, which is characterized by long line distances and large separations between generation and load, and, also, improve the quality of the service, has led EVN to devote significant amounts of talent and resources to the implementation of smart-grid technologies in the country.

In addition to an extended population of Substation Automation Systems (SAS), at the core of this program is the deployment of a vast Wide Area Monitoring System (WAMS) aimed at improving power system performance and reliability.

The plan and scope and the expected applications encompassed by this effort are illustrated in Figs. 3.12 and 3.13, respectively.

This is a two-phase program. The expected WAMS architectures in each one of these phases are illustrated in Figs. 3.14 and 3.15.

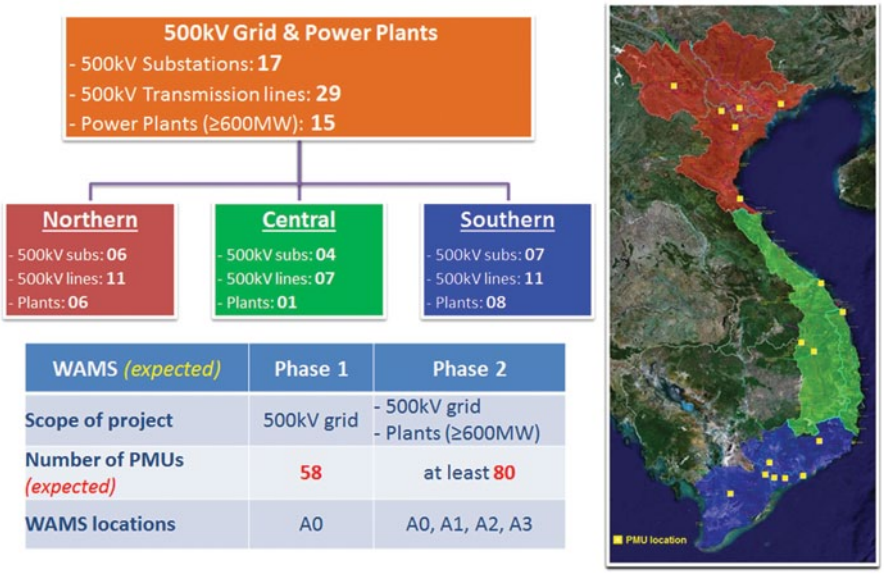

WAMS *(expected)*	Phase 1	Phase 2
Scope of project	500kV grid	- 500kV grid - Plants (≥600MW)
Number of PMUs *(expected)*	58	at least 80
WAMS locations	A0	A0, A1, A2, A3

Fig. 3.12 Plan and scope of the expected WAMS model in Vietnam

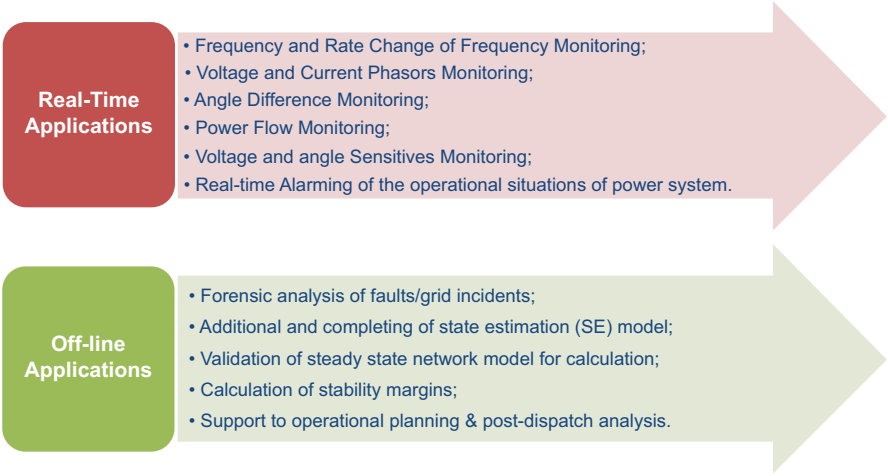

Fig. 3.13 Expected WAMS applications in Vietnam

3.4.2 Real-Time Monitoring of Available Power Transfer Capability Across Long Transmission Corridors

Among the key objectives of the ongoing WAMS effort in Vietnam, which generally aims at improving performance and reliability, is the need to address the fact that one of the primary causes of wide-area disruptions in the current EVN power system is the existence of long transmission corridors that are susceptible to voltage and angle instabilities when major unbalances between load and generation take place.

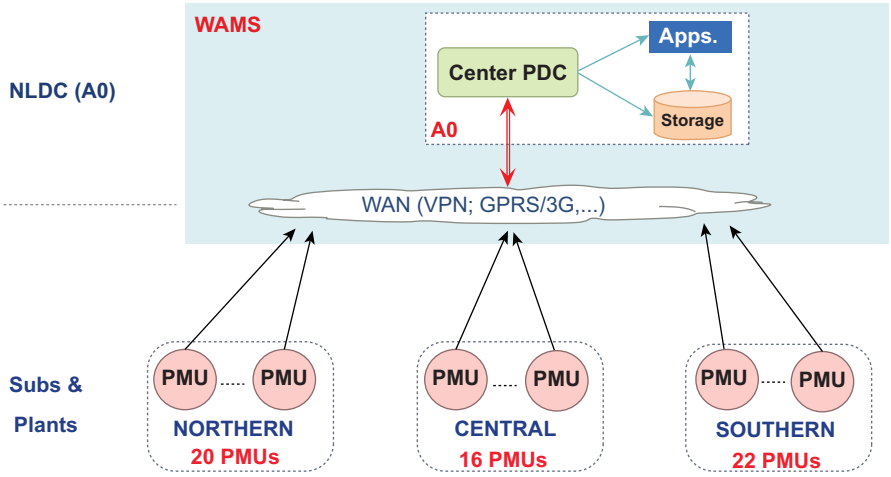

Phase 1:

- Monitor all 500kV Vietnam Grids (including lines, substations and power plants)
- Number of PMUs (expected): 58

Fig. 3.14 WAMS architecture implementation in Vietnam—Phase 1

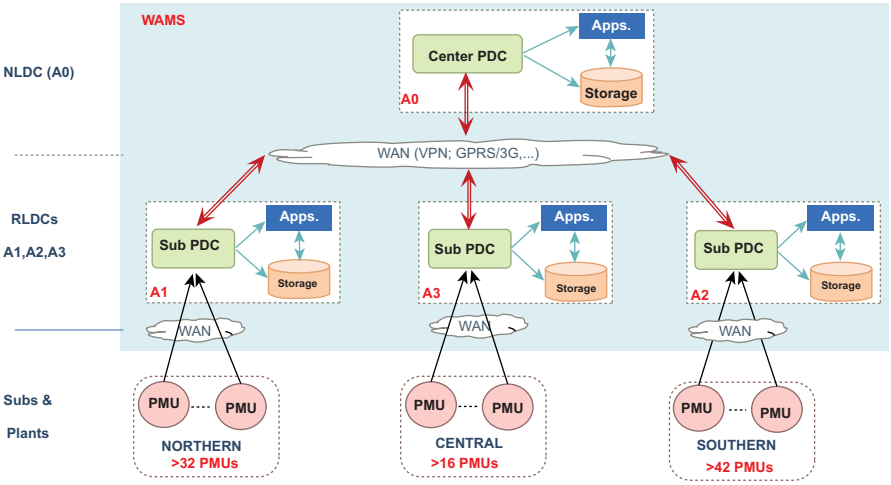

Phase 2:

- Monitor all 500kV Vietnam Grids and power plants with the capacity is over 600MW
- Number of PMUs (expected): over 80

Fig. 3.15 WAMS architecture implementation in Vietnam—Phase 2

3.4.2.1 Classical Concepts in the Context of the Synchrophasor Technology

Quoting from the classical steady-state stability theory, the real power transfer across a transmission line between two adjacent network buses is determined by the voltage magnitudes at each bus, the phase angle difference between them, and the line reactance (Crary 1955; Anderson and Fouad 1990; Venikov 1977).

Accordingly, the real power transfer between the two bus terminals of a transmission line, say A and B, is calculated with the following equation:

$$P = \frac{V_A \times V_B}{X_L} \sin \delta,$$

where P is the real power transfer, X_L is the transmission line reactance between the two buses, δ is the phase angle difference across the transmission line, and V_A and V_B are the bus voltage magnitudes at the terminals of the transmission line.

The amount of maximum power that can be transferred across the line, or its total MW transfer capability, is given by

$$P_{max} = \frac{V_A \times V_B}{X_L},$$

and the line's reserve margin (available transmission capability) $P_{marg\%}$ of the line is calculated as:

$$P_{marg\%} = \frac{P_{max} - P}{P_{max}} \times 100.$$

From these equations, the total and available transfer capabilities across the transmission line can be computed in real time by using the voltage and current synchrophasor data, respectively, collected at the lines' terminals. Three additional metrics can also be defined as shown in Figs. 3.16, 3.17, 3.18.

3.4.2.2 Demonstration of the Synchrophasor Technology on the Vietnamese 500-kv Transmission System

A demonstration of the synchrophasor technology developed in Vietnam[11] was recently conducted at EVN. The functionality, architecture, data flow, and alarm blocks of the application (SmartWAMS) are illustrated schematically in Figs. 3.19, 3.20, 3.21.

The model used for simulation encompassed 17 substations of the Vietnamese 500-kV transmission grid.

[11] The synchrophasor technology was introduced in 2012 in Vietnam by Advanced Technical Systems Co. Ltd (ATS) under the trade name SmartWAMS (patent pending).

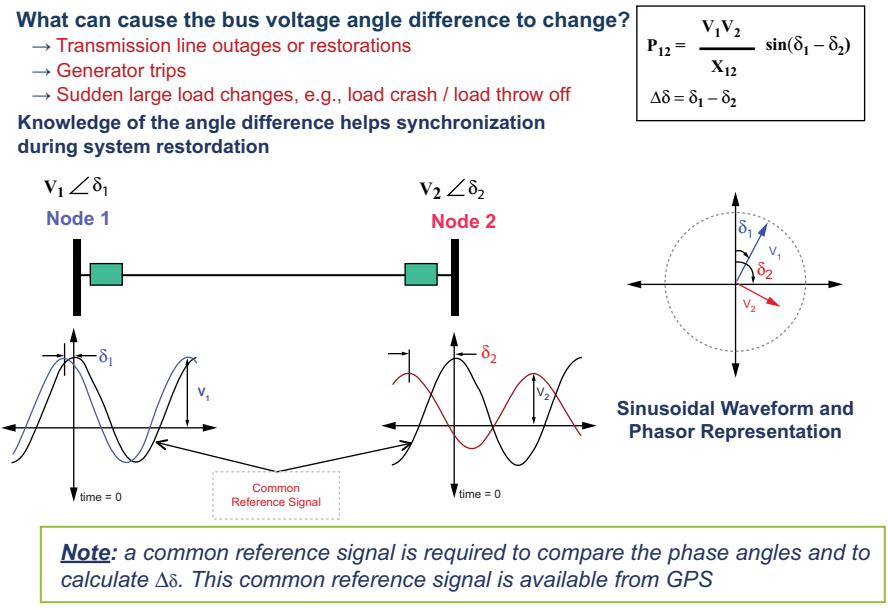

Fig. 3.16 Voltage angle difference concept in synchrophasor technology

- ΔV/ΔP is the change in voltage as a function of the power flow (MW)
- ΔV/ΔP increases as system approaches the collapse region identified as the Nose Point
- Voltage sensitivity allows:
  - → Early warning of deteriorating voltage stability
  - → Indicate "How far are we from the voltage collapse region?"
  - → Determine the voltage stability margin
  - → Identify "When a nearby transmission line or substation trips"

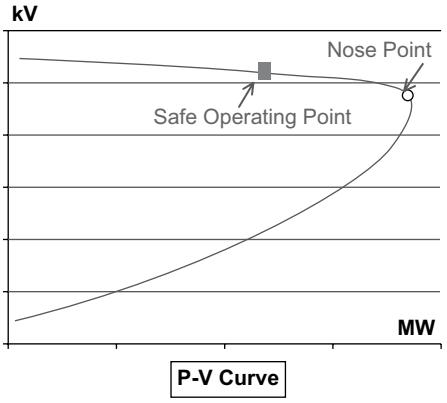

Fig. 3.17 Voltage sensitivity concept

- $\Delta\delta/\Delta P$ is the chnge in angle as a function of the power flow (MW)
- $\Delta\delta/\Delta P$ increases as system approache P_{max1} (the maximum power that can be transmitted)
- Angle Sensitivity allows:
  - → Early warning of deteriorating angle stability
  - → Assessing of the steady state stability
  - → Identify "When a nearby transmission line or substation trips"

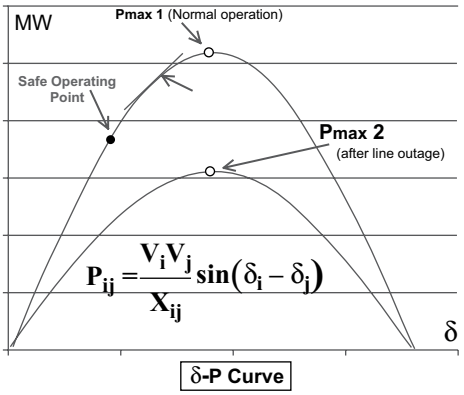

Fig. 3.18 Angle sensitivity concept

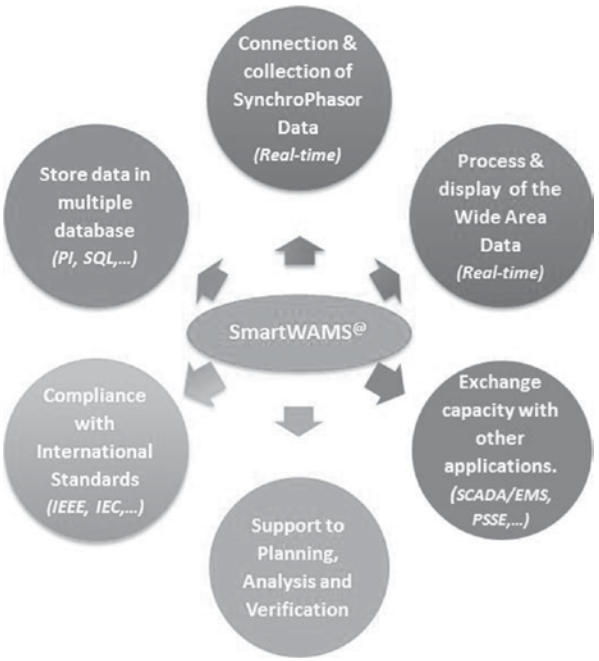

Fig. 3.19 SmartWAMS functionality

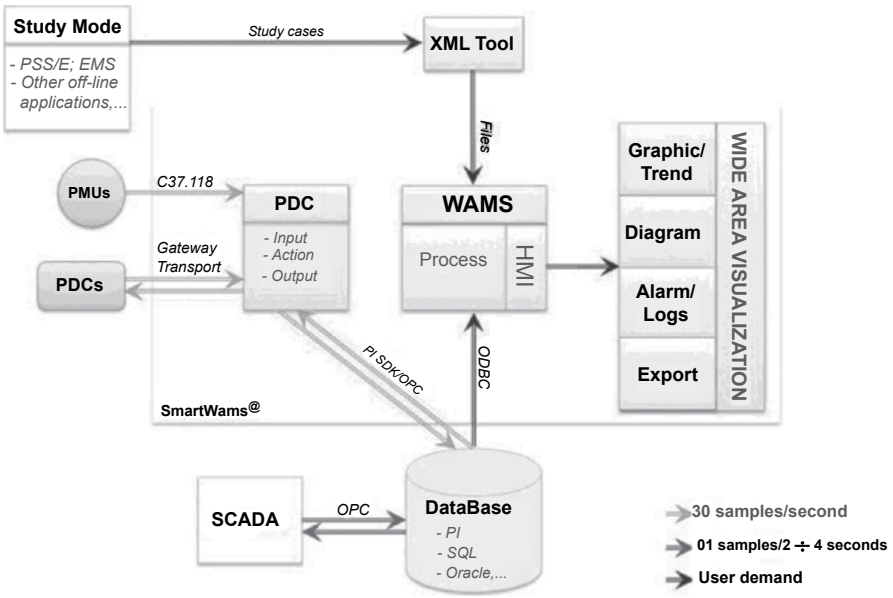

Fig. 3.20 SmartWAMS architecture and dataflow

Fig. 3.21 SmartWAMS visualization alarm blocks

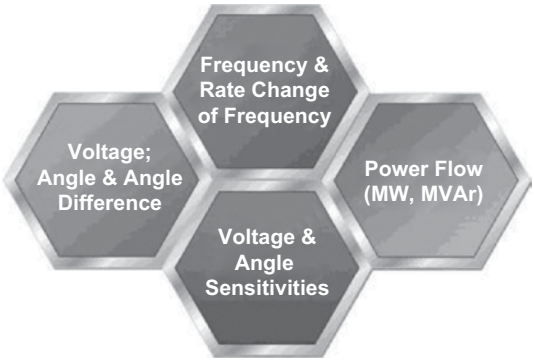

Two demo scenarios were run as follows:

- Scenario 1: running the test with the actual data.
- Scenario 2: running test with solved cases developed with the PSS/E software.

Each scenario included both normal operation conditions (Case 1) and the outage of the 500-kV transmission line PLEIKU—DAKNONG (Case 2).

Some illustrative interfaces and representative results of the simulations are illustrated in Figs. 3.22, 3.23, 3.24, 3.25.

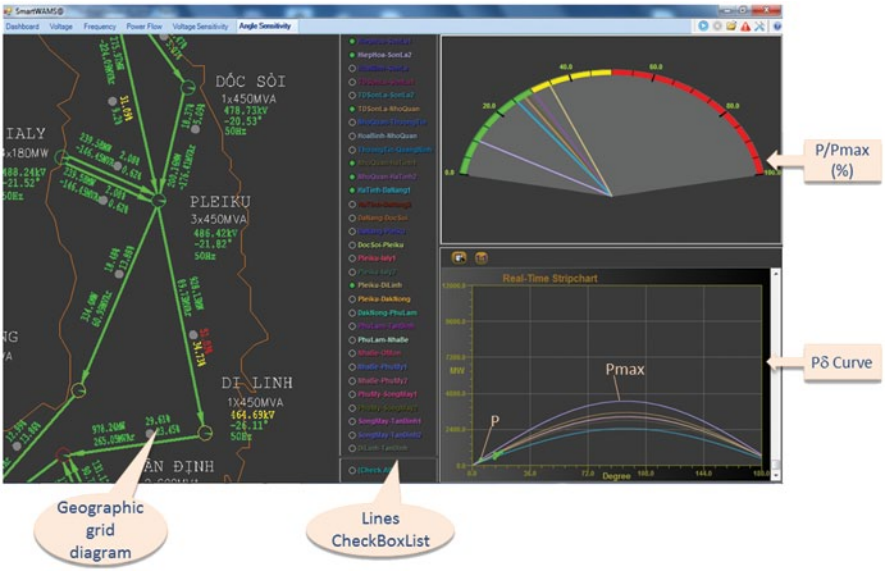

Fig. 3.22 SmartWAMS angle sensitivity displays

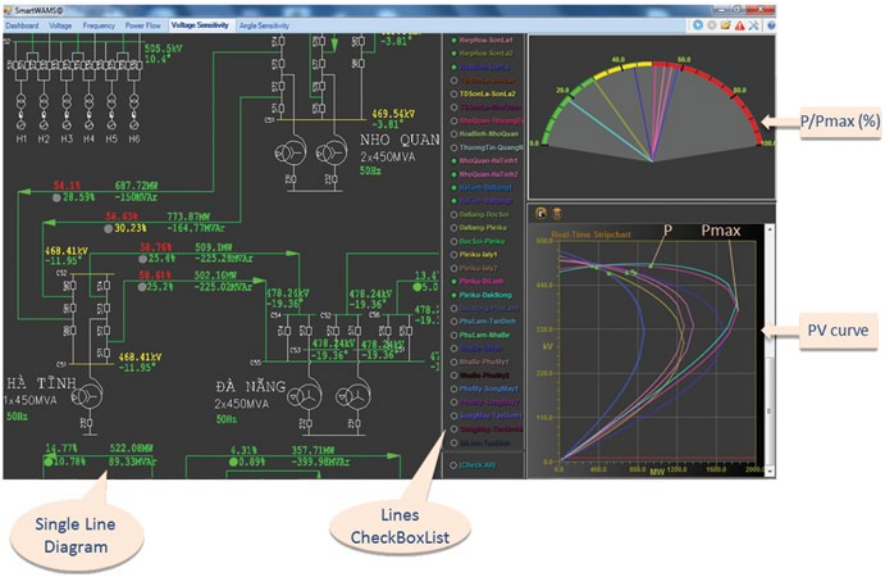

Fig. 3.23 SmartWAMS voltage sensitivity displays

Fig. 3.24 SmartWAMS angle sensitivity displays before and after the outage

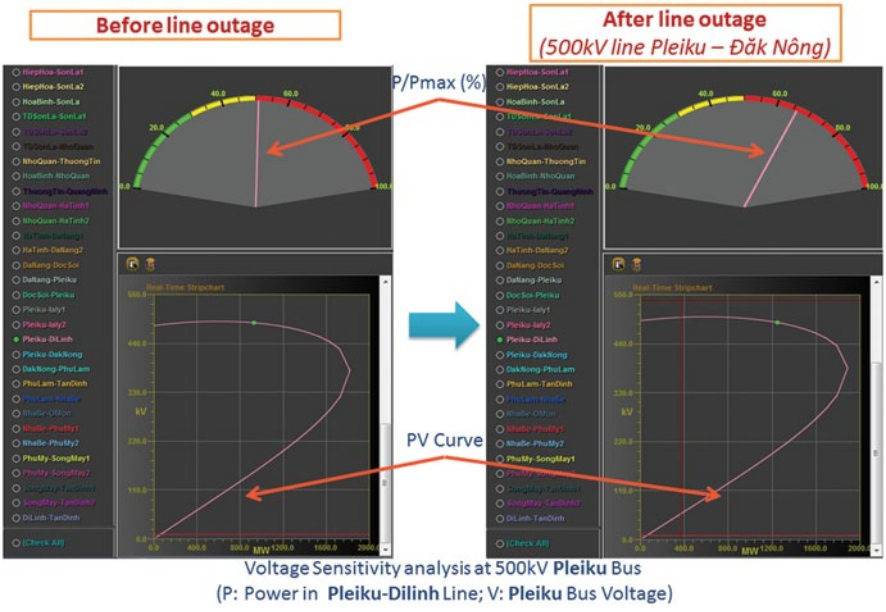

Fig. 3.25 SmartWAMS voltage sensitivity displays before and after the outage

3.5 Conclusions

This chapter addressed several practical aspects of performing steady-state stability assessment in real time. The application validation for accuracy and reliability, which is of paramount importance, has been covered in detail and illustrated with practical experience results obtained by two early users of QuickStab—ETESA, in Panama, and NLDC, in Vietnam. At the time when these tests were performed, ETESA and NLDC were using QuickStab in real time in system dispatching functions and off-line in operations scheduling and market clearing functions. The application validation results confirmed the theory and are consistent with earlier experience with this technology.

The deployment of the steady-state stability assessment in energy control centers was illustrated with an actual example that reflects the benefits of the online monitoring of the risk of blackout via speedometer charts and by trending the distance to instability as it evolves in real time. At the utility site selected for this purpose, the stability computations have been seamlessly integrated with the real-time system by the SCADA/EMS provider.

The potential to use synchrophasor technologies to track voltage and angle stability sensitivities across long transmission lines was also discussed and illustrated with practical results obtained recently in Vietnam. According to the Vietnamese operational experience, the synchronized phasor measurements, which are ideal for monitoring the dynamic power system performance especially during high-stress operating conditions, should be viewed as a complement to, rather than a replacement of, conventional SCADA/EMS tools.

References

Anderson PM, Fouad AA (1990) Power system control and stability. The Iowa University Press, Ames

Arnold L, Hajagos J (2009) LIPA implementation of real-time stability monitoring in a CIM compliant environment. Paper PSE-09PSCE0253 presented at the real-time stability assessment in modern power system control centers panel, IEEE power systems conference & exposition 2009 (IEEE PSCE'09), Seattle, WA, March 15–18, 2009

Avila-Rosales R, Giri J (2004) Extending EMS capabilities to include on-line stability assessment. Paper 04PS0371 presented at the real-time stability challenge panel session, power systems conference and exposition 2004, New York, New York, 10–13 Oct 2004

Campeanu HS, L'Helguen E, Assef Y, Vidal N, Savulescu SC (2006) Real-time stability monitoring at Transelectrica. Paper PSCE06-1288 presented at the real-time stability applications in modern SCADA/EMS panel, IEEE power systems conference & exposition 2006 (IEEE PSCE'04), Atlanta, GA, Oct 29–Nov 2, 2006

Crary S (1955) Power System Stability. Steady-State Stability, General Electric Series, Vol. I: third printing, October 1955

Dimo P (1961) Etude de la stabilité statique et du réglage de tension. Revue Générale de l'Electricité (Paris) 70(11):552–556

Dimo P (1975) Nodal analysis of power systems. Abacus Press, Kent

Dy Liacco TE, Savulescu SC, Ramarao KV (1978) An On-line topological equivalent for a power system, IEEE transactions on power systems, PAS-97, pp 1550–1563

Gonzalez LA (2003) Post-facto analysis of a near-Blackout event. 7th international workshop on power control centers, May 26–28, 2003, Orisei, Italy

IEEE (1982) IEEE PES task force on terms and definitions, proposed terms and definitions for power system stability, IEEE Transactions on Power Systems, PAS-101, No. 7, July 1982

IEEE/CIGRE (2004) IEEE/CIGRE joint task force on stability terms and definitions, definition and classification of power system stability. IEEE, transactions on power systems, vol. 19, no. 2, May 2004, pp 1387–1401

Kundur P (1999) Introduction to techniques for power system stability search. A special publication of the Power System Dynamic Performance Committee of the IEEE PES, TP-138-0, pp 1–3

Magnien M (1964) Rapport spécial du Groupe 32 Conception et Fonctionnement des Réseaux. Conférence Internationale des Grands Réseaux Electriques à Haute Tension, CIGRE Session 1964

Moraite G, Ionescu S, Feldmann S, Chenzbraun I (1966) Problèmes soulevés par la stabilité statique des réseaux bouclés. Conférence Internationale des Grands Réseaux Electriques à Haute Tension, CIGRE Session 1966

NERC (2000) Policy 9—reliability coordinator procedures, version 2. Approved by Board of Trustees 7 Feb2000

Oatts ML, Erwin SR, Hart JL (1990) Application of the REI equivalent for operations planning analysis of interchange schedules. IEEE transactions on power systems, 5, no. 2, May 1990, pp 547–555

Pomarleanu M, Savulescu SC (2009) Detection and evaluation of stability constrained transmission paths. In: Real-time stability assessment in modern power system control centers (Savulescu SC ed). Wiley and IEEE Press, New York, New York, Jan 2009

Sauer PW, Pai MA (1990) Power system steady-state stability and the load-flow Jacobian. IEEE transactions on power systems, 5, T-PWRS-4, pp 1374–1383

Savulescu SC (1981) Equivalents for security analysis of power systems. IEEE transactions on power systems, PAS-100, pp 2672–2682

Savulescu SC (2004) A metric for quantifying the risk of blackout. Paper 04PS0294 presented at the real-time stability challenge panel session, power systems conference and exposition 2004, New York, New York, 10–13 Oct 2004

Savulescu SC (2005) Fast assessment of the distance to instability. Theory and implementation. In: Real time stability in power systems. Springer, Norwell

Savulescu SC (2009a) Dimo's approach to steady-state stability assessment: methodology overview and algorithm validation (co-author). In: Real-time stability assessment in modern power system control centers (edited by Savulescu SC). Wiley and IEEE Press, New York, NY, USA, pp 320–353

Savulescu SC (2009b) Real-time stability assessment in modern power system control centers (ed). Wiley and IEEE Press, New York, New York

Tinney WF, Powell WI (1977) The REI Approach to power network equivalents, PICA'77 conference, May 1977, Toronto, Canada

Venikov VA (1977) Transient processes in electrical power systems (edited by Stroyev VA, English translation). MIR Publishers, Moscow

Venikov VA, Stroev VA, Idelchick VI, Tarasov VI (1975) Estimation of electrical power system steady-state stability. IEEE transactions on power systems, PAS-94, 3, pp 1034–1041

Vergara JS, Gonzalez LA, Savulescu SC, 2005, Practical experience with Dimo's steady-state stability assessment method in Panama. Energetica 53(9):330–337

Vickovic D, Eichler R (2009) Real-time stability monitoring at the independent system operator in Bosnia and Herzegovina. In: Real-time stability assessment in modern power system control centers. Wiley and IEEE Press, New York, New York

Virmani S, Vickovic D, Savulescu SC (2007) Real-time calculation of power system loadability limit. Paper no. 576 presented at the Powertech 2007 conference, July 1–5, 2007, Lausanne, Switzerland

Vournas CD, Sauer PW, Pai MA (1996) Relationships between voltage and angle stability of power systems. Electr Power Energy Syst 18(8):493–500 (Elsevier Science Ltd.)